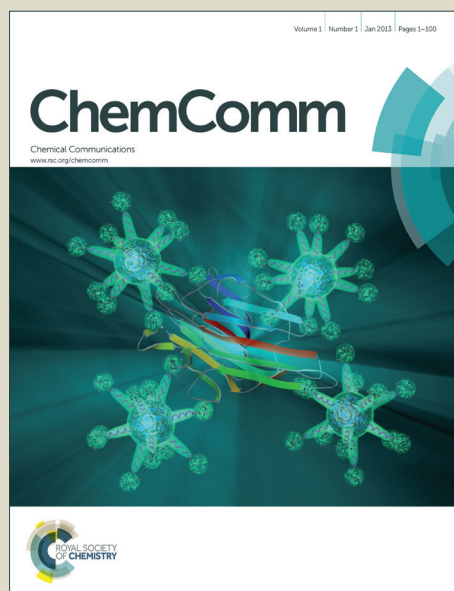


ChemComm

Accepted Manuscript



This is an *Accepted Manuscript*, which has been through the Royal Society of Chemistry peer review process and has been accepted for publication.

Accepted Manuscripts are published online shortly after acceptance, before technical editing, formatting and proof reading. Using this free service, authors can make their results available to the community, in citable form, before we publish the edited article. We will replace this *Accepted Manuscript* with the edited and formatted *Advance Article* as soon as it is available.

You can find more information about *Accepted Manuscripts* in the [Information for Authors](#).

Please note that technical editing may introduce minor changes to the text and/or graphics, which may alter content. The journal's standard [Terms & Conditions](#) and the [Ethical guidelines](#) still apply. In no event shall the Royal Society of Chemistry be held responsible for any errors or omissions in this *Accepted Manuscript* or any consequences arising from the use of any information it contains.

Cite this: DOI: 10.1039/c0xx00000x

www.rsc.org/xxxxxx

ARTICLE TYPE

Aptasensors Based on Supramolecular Structures of Nucleic Acid-Stabilized Ag Nanoclusters

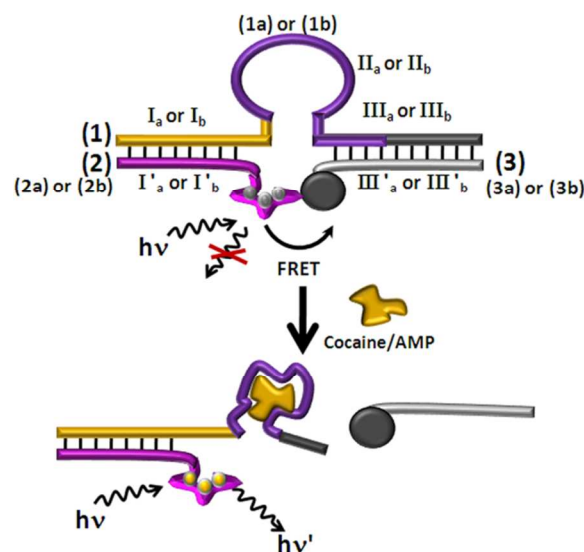
Etery Sharon[‡], Natalie Enkin[‡], H. Bauke Albada and Itamar Willner^{*}

Received (in XXX, XXX) Xth XXXXXXXXX 20XX, Accepted Xth XXXXXXXXX 20XX

DOI: 10.1039/b000000x

Two-sized luminescent nucleic acid-functionalized Ag nanoclusters (NCs) are implemented for the analysis and multiplexed detection of adenosine monophosphate, AMP, and of cocaine using aptamer-ligand complexes.

10 Nucleic acid-stabilized metal nanoclusters, and particularly, Ag⁰ nanoclusters (NCs) attract recent scientific interest due to their unique luminescence properties.^{1, 2} It was found that cytosine-rich nucleic acids stabilize Ag NCs and sequence-specific single-stranded or duplex stabilized Ag NCs were reported.³⁻⁷ The
15 luminescence spectra of the Ag NCs were found to be controlled by the sizes of the NCs and by the nucleic acid sequence capping the NCs. Besides tunable luminescence properties of Ag NCs, they reveal additional interesting photophysical or chemical properties, such as high luminescence quantum yields,
20 photostability against bleaching, solubility in aqueous environments, biocompatibility and low cytotoxicity. The unique optical properties of nucleic acid-stabilized Ag NCs turned them into ideal optical labels for the development of different sensors⁸ and for bioimaging.^{9,10} For example, nucleic acid stabilized Ag
25 NCs were applied for the optical detection of metal ions¹¹ such as Hg²⁺, or Cu²⁺, for the sensing of explosives,¹² such as picric acid, TNT or RDX, and for the analysis of thiols such as cysteine or glutathione.¹³ Also, Ag NCs were applied as luminescent labels for the detection of DNA,^{14,15} micro-RNA,¹⁶ and for probing
30 enzyme activities such as glucose oxidase or tyrosinase.¹⁷ The tunable luminescence features of Ag NCs were implemented to develop multiplexed assays for the analysis of DNAs.¹⁸ Although numerous sensing platforms that utilize aptamers for the analysis of low-molecular-weight substrates or of proteins were
35 reported,^{19, 20} only a few examples have reported the use of Ag NCs as optical label for the detection of aptamer-substrate complexes. For example, the analyte-induced self-assembly of aptamer subunits tethered to sequence-specific nucleic acids that stabilize Ag NCs was reported as a means to detect cocaine or
40 adenosine monophosphate (AMP).²¹ This method required, however, the synthesis of the Ag NCs after the formation of the aptamer-analyte complexes. Similarly, nucleic acid-stabilized Ag NCs were tethered to aptamer recognition sequences, and the nucleic acid conjugates were adsorbed onto graphene oxide,
45 where the luminescence of the Ag NCs was quenched by the graphene oxide supports. The desorption of the conjugated from the graphene oxide through the formation of the aptamer-substrate complexes triggered-on the luminescence of



50 Fig. 1 Schematic configuration of the aptamer-ligand sensing module consisting of the hairpin probe/the nucleic acid-stabilized Ag NCs and the quencher-modified nucleic acid. The ligand induced formation of the aptamer-ligand complex leads to the separation of the nanostructure and to the luminescence of the
55 Ag NCs.

the NCs.¹⁸ This latter method reveals, however, limited sensitivity due to the need to apply relatively high concentration of the analyte to desorb the aptamer from the graphitic matrix. Although substantial progress in developing Ag NCs-based
60 aptasensors was demonstrated, the development of novel Ag NCs-based aptasensor platforms, and particularly multiplexed aptasensing assays is important. Here we wish to report on the development of a versatile sensing module for the luminescence detection of aptamer-substrate complexes using different nucleic
65 acid stabilized Ag NCs as luminescent labels. Specifically, we apply the tunable luminescence properties of Ag NCs to demonstrate the multiplexed detection of two analytes (cocaine and adenosine monophosphate, AMP).

The aptamer sensing module is depicted in Figure 1. It
70 includes a hairpin nucleic acid scaffold (1), a nucleic acid-functionalized Ag NCs (2), and a quencher-modified nucleic acid (3). We implement this sensing module for analyzing cocaine or AMP. Accordingly, the sensing modules for sensing the two analytes are designed to include the appropriate constituents. The

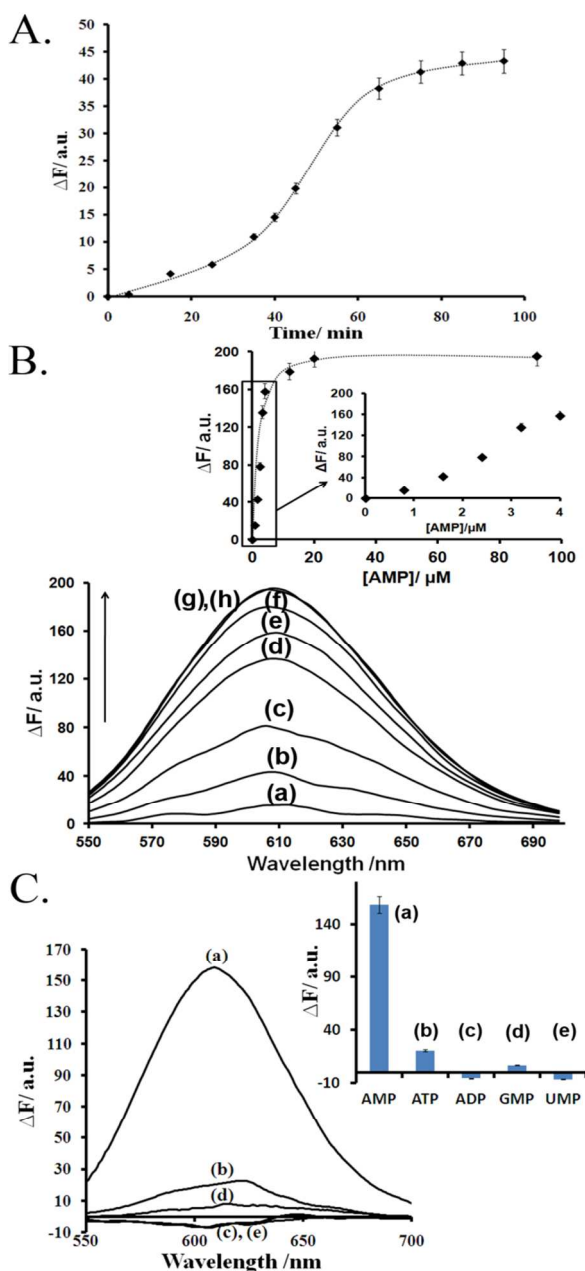


Fig. 2 (A) Time-dependent luminescence changes upon the interaction of the sensing module shown in Figure 1 with AMP, 1.6 μM . (B) Fluorescence spectra corresponding to the analysis of 5 different concentrations of AMP, according to Figure 1: (a) 0.8 μM (b) 1.6 μM (c) 2.4 μM (d) 3.2 μM (e) 4 μM (f) 12 μM (g) 20 μM (h) 92 μM . Spectra recorded after a fixed time-interval of 75 minutes. Inset: Derived calibration curve. (C) Selectivity study corresponding to the analysis of AMP. Luminescence spectra corresponding to the analysis of: (a) AMP 4 μM (b), (c), (d) and (e) ATP, ADP, GMP, UMP, respectively, each 26 μM . Inset: Selectivity results in the form of luminescence changes in bar presentation. The negative ΔF values observed for ADP and UMP are attributed to inefficient quenching of the AgNCs by these nucleotides.

15 hairpin scaffold (**1a**) or (**1b**) are used to construct the cocaine and AMP sensing modules, respectively. Similarly, the luminescent Ag NCs stabilized by the nucleic acids (**2a**) or (**2b**) are implemented as the optical labels to analyze cocaine or AMP, respectively. ESI-mass spectrometry indicated that the

20 (**2a**)-functionalized Ag NCs consist of 4-5 silver atoms. TEM images of the clusters indicated a diameter of ca. 3-5 nm. Similarly, ESI-mass spectrometry analysis showed that the (**2b**)-modified Ag NCs consist of 6-7 Ag atoms, and TEM images indicated ca. 5 nm diameter for the NCs (For details see 25 Supporting Information, Figure S1 and Table S1). Also, the quencher modified nucleic acids, (**3a**) and (**3b**) are used as the functional units for sensing of cocaine or AMP, respectively (quencher = IAbRQSp for (**3a**) and quencher= BHQ2 for (**3b**)). The scaffolds (**1a**) and (**1b**) include in the hairpin domains II_a and 30 II_b , the aptamer recognition sequences for cocaine and AMP, respectively. The domains I_a and I_b in scaffolds (**1a**) and (**1b**) are complementary to the domains I'_a and I'_b associated with the nucleic acids (**2a**) and (**2b**), stabilizing the silver NCs. While I'_a includes the sequence stabilizing the 615 nm luminescent Ag NC 35 ($\lambda_{\text{ex}} = 520 \text{ nm}$), the domain I'_b corresponds to the sequence that stabilizes the 540 nm luminescent Ag NCs ($\lambda_{\text{ex}} = 480 \text{ nm}$). The domains III_a and III_b that are part of (**1a**) and (**1b**) are complementary to the quencher-functionalized sequences III'_a and III'_b associated with (**3a**) and (**3b**), respectively. 40 Accordingly, the hybridization features of the pre-designed functional nucleic acid constituents lead, in the absence of analytes, to the formation of the supramolecular sensing modules composed of (**1a**)/(**2a**)/(**3a**) for sensing of AMP, and of (**1b**)/(**2b**)/(**3b**) for the sensing of cocaine. The close proximity 45 between the Ag NCs and the quencher units in the supramolecular structures leads to the luminescence quenching of the NCs. In the presence of the respective analytes, AMP or cocaine, the hairpin structures open by forming the respective energetically stabilized aptamer-substrate complexes. This leads 50 to the separation of the quencher-modified strands (**3a**) or (**3b**) from the respective supramolecular complexes, resulting in the triggered-on luminescence of the respective Ag NCs ($\lambda_{\text{em}} = 615 \text{ nm}$ for AMP, $\lambda_{\text{em}} = 540 \text{ nm}$ for cocaine). As the degree of opening of the respective hairpins is controlled by the 55 concentration of the analyte (and the time-interval of interaction between the analytes in the sensing modules), the resulting luminescence intensities provide a quantitative output signal for the sensing of the analytes. Furthermore, by mixing of the two sensing modules (**1a**)/(**2a**)/(**3a**) and (**1b**)/(**2b**)/(**3b**), the 60 multiplexed analysis of the two analytes should proceed. It should be noted that a similar sensing module was recently reported by us for the analysis of DNA.²² The present study demonstrates, however, that the aptamer-ligand complex separates the sensing module and leads to effective luminescent aptasensors.

65 Figure 2(A) depicts the time-dependent fluorescence changes upon subjecting the sensing module (**1a**)/(**2a**)/(**3a**) to a fixed concentration of 1.6 μM of AMP. The luminescence spectra are intensified with time, consistent with the time-dependent dynamic opening of the hairpin domain of (**1a**). The system reaches a 70 saturation equilibrium value after ca. 90 min. minutes. We selected a fixed time-interval of 75 min. for the interaction between the sensing module and different concentrations of AMP. Figure 2(B) shows the changes of the luminescence spectra of the system upon analyzing different concentrations of AMP. 75 As the concentration of AMP increases the luminescence at $\lambda_{\text{em}} = 615 \text{ nm}$ is intensified, consistent with the higher degree of separation of the sensing module. Figure 2(B) inset, shows the

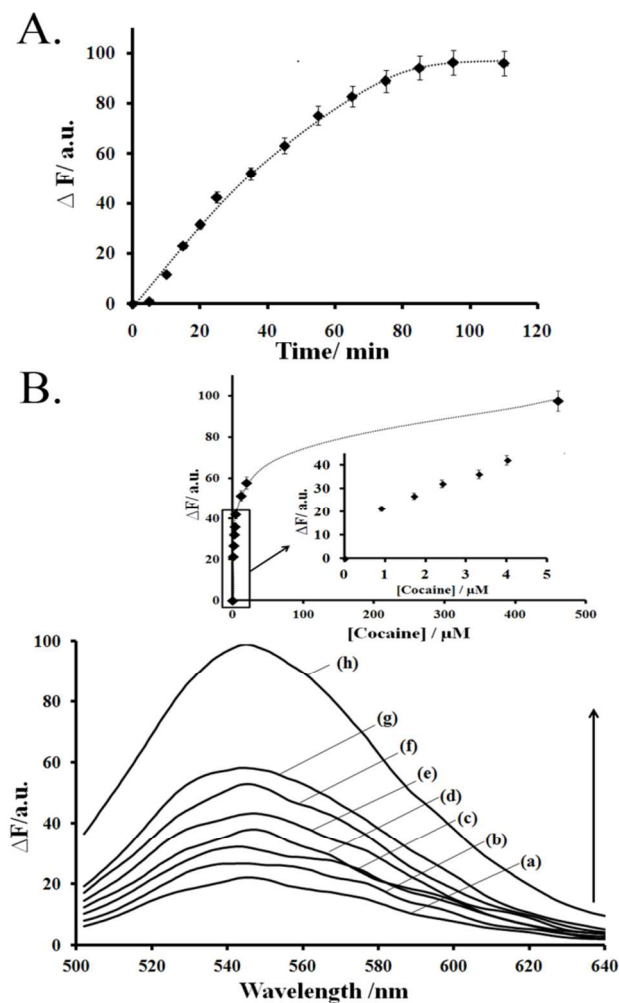


Fig. 3 (A) Time-dependent luminescence changes upon the interaction of the sensing module shown in Figure 1 with cocaine, 460 μM . (B) Luminescence spectra corresponding to the analysis of different concentrations of cocaine, according to Figure 1: (a) 0.9 μM (b) 1.7 μM (c) 2.4 μM (d) 3.3 μM (e) 4 μM (f) 12 μM (g) 20 μM (h) 460 μM . Spectra were recorded after a fixed time-interval of 95 Minutes.

resulting calibration curve. The detection limit for analyzing AMP corresponds to 0.4 μM . Impressive selectivity is observed for analyzing AMP by the sensing module, Figure 2(C). In these experiments the sensing module (1)/(2)/(3) was interacted with 4 μM of AMP and with 26 μM of any of the monophosphorylated nucleotides ATP, GMP, UMP, CMP and the resulting fluorescence changes were compared to the fluorescence changes generated by 4 μM of AMP (6.5-fold lower concentration of AMP!). The results reveal high selectivity and only minute fluorescence changes are generated by the foreign phosphorylated nucleotides that are not recognized by the aptamer.

The analysis of cocaine by the sensing module (1b)/(2b)/(3b) has been then applied for the luminescence detection of cocaine. Figure 3(A) depicts the time-dependent luminescence changes of the system, at $\lambda_{\text{em}} = 540 \text{ nm}$, upon subjecting the sensing module to a constant concentration of cocaine, $4.6 \times 10^{-4} \text{ M}$. As the time of interaction between the sensing module and cocaine is intensified, the luminescence generated by the system is intensified, and it levels off to a saturation equilibrium value after

ca. 95 min. The increase in the luminescence of the system represents the dynamics of opening of the hairpin unit of (1b) by cocaine and the concomitant separation of (3b) from the supramolecular sensing module. We selected a fixed time interval of 85 min for interacting cocaine with the sensing module. Figure 3(B) shows the changes in the luminescence generated by the system upon analyzing different concentrations of cocaine for a fixed time interval of 85 min, by the sensing module (1b)/(2b)/(3b). Figure 3(B), inset, depicts the derived calibration curve. The system enabled the analysis cocaine with a detection limit that corresponds to 0.3 μM . For the selective analysis of cocaine see Supporting Information, Figure S2 and accompanying discussion.

The analysis of AMP by the sensing module (1a)/(2a)/(3a) has applied 615 nm luminescent Ag NCs as optical readout label, whereas the cocaine sensing module has implemented the 540 nm luminescent Ag NCs as optical readout output. Thus, by mixing the two modules (1a)/(2a)/(3a) and (1b)/(2b)/(3b) the multiplex analysis of the two targets AMP and/or cocaine may proceed, Figure 4(A). The luminescence intensities of the mixture of the two modules upon the multiplexed analysis of AMP and cocaine are depicted in Figure 4(B). Figure 4(B), panel I depicts the luminescence intensities of the mixture of the two-sensor modules upon interaction with only AMP 1.4 μM . Luminescence changes at $\lambda = 615 \text{ nm}$ are observed, while no luminescence changes are observed at $\lambda = 540 \text{ nm}$, consistent with the selective sensing of AMP. Figure 4(B), panel II, shows the fluorescence intensities of the multiplexed sensing platform upon interaction with cocaine, 3 μM . Only the luminescence at $\lambda = 540 \text{ nm}$ is triggered on indicating the successful selective detection of the cocaine analyte. Figure 4(B), panel III shows the luminescence intensities of the system upon interaction with the two targets, AMP and cocaine. The resulting luminescence bands at $\lambda = 615 \text{ nm}$ and $\lambda = 540 \text{ nm}$ reveal the multiplexed analysis of the two analytes. It should be noted that the luminescence of the AgNCs, used in the present study was almost unchanged with a time-interval of one week (<10% decrease in the luminescence intensities).

The list of nucleic acids sequences used in the study include:

(1a) 5'-CTC TGC TCG ACG GAT TCC TCC TGG GGG AGT ATT GCG GAG GGA GGA AGG TTA AGT GT-3'

(2a) 5'-ACC CGA ACC TGG GCT ACC ACC CTT AAT CCC CAA TCC GTC GAG CAG AG-3'

(3a) 5'-ACA CTT AAC CTT TTT- IAbRQSp -3'

(1b) 5'-GCT GCA GAA TGG GAT CTT CAT GAC AAG GAA AAT CCT TCA ATG AAG TGG GTC AAT TAT-3'

(2b) 5'-CCC TTC CTT CCT TCC AAC CAA CCC ATC CCA TTC TGC AGC-3'

(3b) 5'-ATA ATT GAC CCA TTT-BHQ2 -3'

Conclusions

In conclusion, the present study has introduced a new versatile construct of a sensing module for the analysis of aptamer-substrate complexes using Ag NCs as optical readout labels. By using two different Ag NCs, exhibiting tunable luminescence properties, the multiplexed analysis of two different aptamer-substrate complexes was demonstrated.

Cite this: DOI: 10.1039/c0xx00000x

www.rsc.org/xxxxxx

ARTICLE TYPE

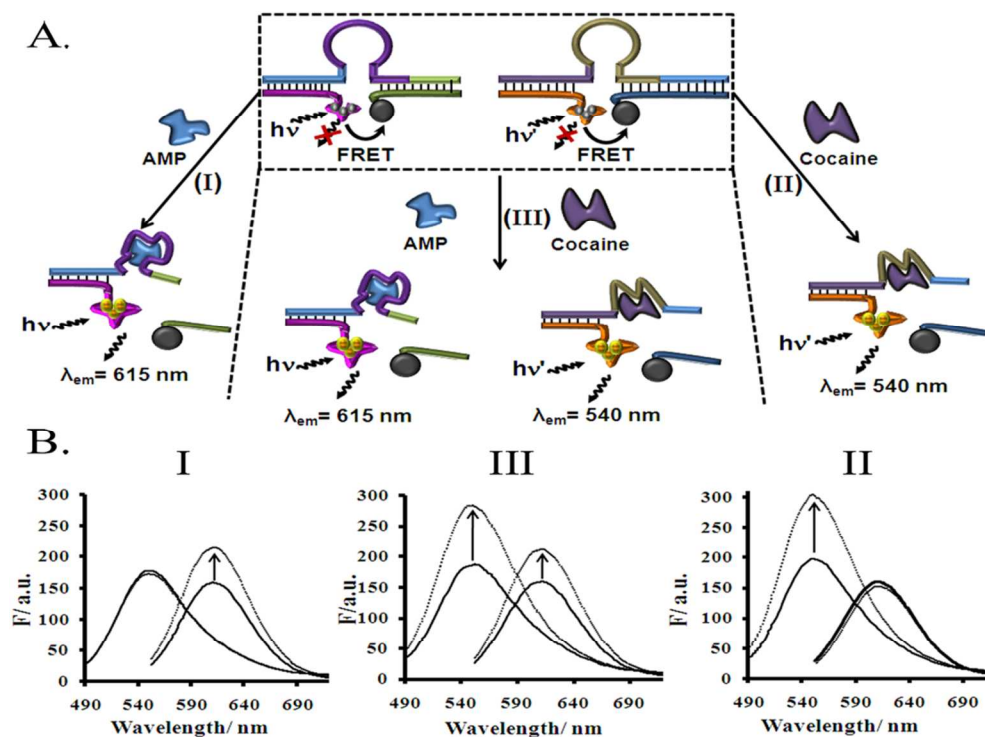


Fig. 4 (A) Scheme for the multiplexed analysis of cocaine and AMP using a mixture of different luminescent Ag NCs. (B) Fluorescence intensities of the multiplexed sensing modules mixture subjected to: panel I: AMP, 1.4 μ M; panel II: cocaine, 3 μ M; panel III: AMP, 1.4 μ M and cocaine, 3 μ M.

Notes and references

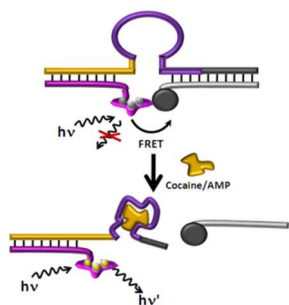
^a E. Sharon, N. Enkin, Prof. I. Willner. Institute of Chemistry, The Center for Nanoscience and Nanotechnology. The Hebrew University of Jerusalem, Jerusalem 91904 (Israel). Fax: (+972) 2-652771
E-mail: willner@vms.huji.ac.il

[†] Electronic Supplementary Information (ESI) available: [detailed experimental section for the different systems is provided]. See DOI: 10.1039/b000000x/

[‡] E.S. and N.E. contributed equally to this work. This research is supported by the Israel Science Foundation.

- 1 E. G. Gwinn, P. O'Neill, A. J. Guerrero, D. Bouwmeester, D. K. Fygenson, *Adv. Mater.*, 2008, **20**, 279-283.
- 2 C. I. Richards, S. Choi, J. C. Hsiang, Y. Antoku, T. Vosch, A. Bongiorno, Y.L. Tzeng, R. M. Dickson, *J. Am. Chem. Soc.*, 2008, **130**, 5038-5039.
- 3 J. Sharma, R. C. Rocha, M. L. Phipps, H. Yeh, K. A. Balatsky, D. M. Vu, A. P. Shreve, J. H. Werner, J. S. Martinez, *Nanoscale*, 2012, **4**, 4107-4110.
- 4 P. R. O'Neill, L. R. Velazquez, D. G. Dunn, E. G. Gwinn, D. K. Fygenson, *J. Phys. Chem. C*, 2009, **113**, 4229-4233.
- 5 J. T. Petty, J. Zheng, N. V. Hud, R. M. Dickson, *J. Am. Chem. Soc.*, 2004, **126**, 5207-5212.
- 6 T. Vosch, Y. Antoku, J. C. Hsiang, C. I. Richards, J. I. Gonzalez, R. M. Dickson, *Proc. Natl. Acad. Sci. U.S.A.*, 2007, **104**, 12616-12621.
- 7 C. M. Ritchie, K. R. Johnsen, J. R. Kiser, Y. Antoku, R. M. Dickson, J. T. Petty, *J. Phys. Chem. C*, 2007, **111**, 175-181.
- 8 B. Han, E. Wang, *Anal. Bioanal. Chem.*, 2012, **402**, 129-138.
- 9 S. Choi, R. M. Dickson, J. Yu, *Chem. Soc. Rev.*, 2012, **41**, 1867-1891.

- 10 A. Latorre, Á. Somoza, *ChemBioChem*, 2012, **13**, 951-958.
- 11 Y.-T. Su, G.-Y. Lan, W.-Y. H.-T. Chen, Chang, *Anal. Chem.*, 2010, **82**, 8566-8572.
- 12 N. Enkin, E. Sharon, E. Golub, I. Willner, *Nano Lett.*, 2014, **14**, 4918-4922.
- 13 W.-Y. Chen, G.-Y. Lan, H.-T. Chang, *Anal. Chem.*, 2011, **83**, 9450-9455.
- 14 J. T. Petty, B. Sengupta, S. P. Story, N. N. Degtyareva, *Anal. Chem.*, 2011, **83**, 5957-5964.
- 15 W. Guo, J. Yuan, Q. Dong, E. Wang, *J. Am. Chem. Soc.*, 2010, **132**, 932-934.
- 16 P. Shah, A. Rørvig-Lund, S. B. Chaabane, P. W. Thulstrup, H. G. Kjaergaard, E. Fron, J. Hofkens, S. W. Yang, T. Vosch, *ACS Nano*, 2012, **6**, 8803-8814.
- 17 X. Liu, F. Wang, A. Niazov-Elkan, W. Guo, I. Willner, *Nano Lett.*, 2013, **13**, 309-314.
- 18 X. Liu, F. Wang, R. Aizen, O. Yehezkeli, I. Willner, *J. Am. Chem. Soc.*, 2013, **135**, 11832-11839.
- 19 M. Levy, S. F. Cater, A. D. Ellington, *ChemBioChem*, 2005, **6**, 2163-2166.
- 20 E. Sharon, R. Freeman, I. Willner, *Anal. Chem.*, 2010, **82**, 7073-7077.
- 21 Z. Zhou, Y. Du, S. Dong, *Biosensors and Bioelectronics*, 2010, **28**, 33.
- 22 N. Enkin, F. Wang, E. Sharon, H. Bauke Albada, I. Willner, *ACS Nano*, 2014, **8**, DOI: 10.1021/nn504983j.



TOC

A supramolecular DNA nanocluster consisting of Ag NCs allow the
5 luminescent detection and multiplexed analysis of ligand-aptamer
complexes.